Insulin-like Growth Factor 2 Expression Modulates Taxol Resistance and Is a Candidate Biomarker for Reduced Disease-Free Survival in Ovarian Cancer

Gloria S. Huang[1,3,5], Jurriaan Brouwer-Visser[1,3], Marissa J. Ramirez[3], Christine H. Kim[1], Tiffany M. Hebert[2], Juan Lin[4], Hugo Arias-Pulido[6], Clifford R. Qualls[7], Eric R. Prossnitz[8], Gary L. Goldberg[1,5], Harriet O. Smith[1,5], and Susan Band Horwitz[3,5]

Abstract

Purpose: This study was undertaken to examine the role of the insulin-like growth factor (IGF) signaling pathway in the response of ovarian cancer cells to Taxol and to evaluate the significance of this pathway in human epithelial ovarian tumors.

Experimental Design: The effect of Taxol treatment on AKT activation in A2780 ovarian carcinoma cells was evaluated using antibodies specific for phospho-AKT. To study the drug-resistant phenotype, we developed a Taxol-resistant cell line, HEY-T30, derived from HEY ovarian carcinoma cells. IGF2 expression was measured by real-time PCR. A type 1 IGF receptor (IGF1R) inhibitor, NVP-AEW541, and IGF2 small interfering RNA were used to evaluate the effect of IGF pathway inhibition on proliferation and Taxol sensitivity. IGF2 protein expression was evaluated by immunohistochemistry in 115 epithelial ovarian tumors and analyzed in relation to clinical/pathologic factors using the χ^2 or Fisher's exact tests. The influence of IGF2 expression on survival was studied with Cox regression.

Results: Taxol-induced AKT phosphorylation required IGF1R tyrosine kinase activity and was associated with upregulation of IGF2. Resistant cells had higher IGF2 expression compared with sensitive cells, and IGF pathway inhibition restored sensitivity to Taxol. High IGF2 tumor expression correlated with advanced stage ($P < 0.001$) and tumor grade ($P < 0.01$) and reduced disease-free survival ($P < 0.05$).

Conclusions: IGF2 modulates Taxol resistance, and tumor IGF2 expression is a candidate prognostic biomarker in epithelial ovarian tumors. IGF pathway inhibition sensitizes drug-resistant ovarian carcinoma cells to Taxol. Such novel findings suggest that IGF2 represents a therapeutic target in ovarian cancer, particularly in the setting of Taxol resistance. *Clin Cancer Res; 16(11); 2999–3010. ©2010 AACR.*

The high mortality rate of ovarian cancer is due to treatment failure in the setting of recurrent/progressive disease that is unresponsive to chemotherapy. Elucidation of the biological factors underlying drug resistance is critical for the development of more effective treatment. Exposure to diverse chemotherapeutic agents induces alterations in gene expression and in signaling cascades that can mediate resistance. Identifying and targeting these cell-specific adaptive responses represent a rational approach to the development of novel drug combination treatment strategies to circumvent resistance.

The widely used chemotherapeutic agent Taxol is indicated for first-line and subsequent treatment of ovarian carcinoma. On associating with its specific binding site on β-tubulin in the microtubule polymer, Taxol stabilizes microtubules and alters their dynamic properties, thereby perturbing their normal function in spindle assembly, cell division, motility, intracellular trafficking, and signaling (1–5). Several mechanisms of Taxol resistance have been identified, including overexpression of the transporter P-glycoprotein, alterations in tubulin, and aberrant signal transduction pathways and/or cell death pathways (6). Despite these discoveries, there remains a critical need for the development of effective strategies to overcome clinical Taxol resistance.

We and others have shown that Taxol exposure can activate proliferative and antiapoptotic signaling pathways

Authors' Affiliations: Departments of [1]Obstetrics and Gynecology and Women's Health, Division of Gynecologic Oncology and [2]Pathology, Albert Einstein College of Medicine and Montefiore Medical Center; Departments of [3]Molecular Pharmacology and [4]Epidemiology and Population Health, Albert Einstein College of Medicine; [5]Albert Einstein Cancer Center, Bronx, New York and Departments of [6]Internal Medicine, [7]Mathematics and Statistics, and [8]Cell Biology and Physiology and University of New Mexico Cancer Center; University of New Mexico, Albuquerque, New Mexico

Corresponding Author: Gloria S. Huang, Division of Gynecologic Oncology, Albert Einstein College of Medicine and Montefiore Medical Center, 1695 Eastchester Road, Suite 601, Bronx, NY 10461. Phone: 718-405-8082; Fax: 718-405-8087; E-mail: gloria.huang@einstein.yu.edu.

©2010 American Association for Cancer Research.

Translational Relevance

Elucidation of biological factors underlying drug resistance is critical for developing more effective treatments for ovarian cancer. Activation of the serine-threonine kinase AKT, which promotes cellular survival, occurs following Taxol treatment; however, the upstream signaling events have not been thoroughly investigated. In this study, we examined the role of the insulin-like growth factor (IGF) signaling pathway in the response of ovarian cancer cells to Taxol. Taxol-induced AKT phosphorylation required type 1 IGF receptor (IGF1R) activity and was associated with upregulation of IGF2. Resistant cells exhibited increased IGF2 mRNA compared with sensitive cells. IGF pathway inhibition, by IGF1R blockade or IGF2 depletion, restored Taxol sensitivity. High IGF2 expression in ovarian tumors was associated with advanced stage and high grade; patients with high IGF2 tumor expression had reduced disease-free survival. Thus, IGF2 modulates Taxol resistance, and its expression correlates with poor prognosis in patients. These novel findings suggest that IGF2 is a therapeutic target for ovarian cancer.

in cancer cells. For example, cell-specific activation of extracellular signal-regulated kinase (ERK) activity has been observed after Taxol treatment (7). In cells that exhibit Taxol-induced ERK activation, mitogen-activated protein kinase pathway inhibitors potentiate Taxol response *in vitro* and *in vivo* (8). Activation of the serine-threonine kinase AKT, which promotes cellular survival, has also been observed following Taxol treatment of ovarian cancer cells (9). However, the upstream signaling events that initiate Taxol-induced AKT activation have not been thoroughly investigated.

Ovarian carcinoma cells grown in tissue culture secrete insulin-like growth factor 2 (IGF2) and express its major receptor, the type 1 IGF receptor (IGF1R), suggesting a role for autocrine/paracrine IGF2-IGF1R signaling in these cells (10). IGF1R is a transmembrane tyrosine kinase receptor that undergoes autophosphorylation on binding of either IGF1 or IGF2, leading to tyrosine kinase activation. Activated IGF1R initiates an antiapoptotic signaling cascade mediated by increased phosphatidylinositol 3-kinase (PI3K) activity, resulting in activation of the downstream antiapoptotic effector AKT (11, 12). The IGF1R pathway is an attractive candidate for targeted therapy, and several small molecules and antibodies that specifically inhibit IGF1R are undergoing clinical evaluation and may be approved for use in the clinic (13).

For these reasons, the present study was undertaken, to our knowledge the first to examine the role of the IGF signaling pathway in the cellular response of ovarian cancer cells to Taxol treatment, as well as the first to measure

IGF2 protein expression in a sizeable cohort of patients with epithelial ovarian tumors. We report the novel finding that Taxol-induced AKT phosphorylation occurs in an IGF1R-dependent manner and is associated with upregulation of IGF2 mRNA expression. Furthermore, to study the drug-resistant phenotype, we developed a cell line model of acquired Taxol resistance and compared these cells with the parental, chemosensitive cell line. The Taxol-resistant cells exhibit significant upregulation of IGF2 gene expression. IGF pathway inhibition, by IGF1R blockade or IGF2 depletion, restores sensitivity to Taxol in these resistant cells. Furthermore, we assessed IGF2 protein expression levels by immunohistochemistry in 115 primary human epithelial ovarian tumors. High IGF2 expression was significantly associated with invasive carcinoma and disease progression and correlated with shortened interval to disease recurrence. Thus, IGF2 is identified for the first time to be a crucial mediator of Taxol resistance in ovarian carcinoma cells, and its expression in primary epithelial ovarian tumors is associated with poor prognostic factors for recurrence; these findings offer significant potential for clinical application.

Materials and Methods

A2780 and HEY ovarian carcinoma cells were maintained as subconfluent monolayer cultures in RPMI 1640 supplemented with 10% fetal bovine serum (Atlanta) and 1% penicillin-streptomycin (Invitrogen). The Taxol-resistant cell line HEY-T30 was developed in our laboratory by exposure of HEY cells to stepwise escalating concentrations of Taxol over a 6-month period and is maintained in media containing Taxol (30 nmol/L). The IGF1R inhibitor NVP-AEW541, a kind gift from Novartis Pharma AG, is a pyrrolo[2,3-*d*]pyrimidine derivative small molecular weight kinase inhibitor of IGF1R (14).

Immunoblotting and densitometry

Cells were treated as described in the figure legends. Cell lysates were prepared as previously described, and protein concentration was determined by the Lowry method (15). Cell lysates were separated by SDS-PAGE and transferred to nitrocellulose. Equal protein loading was confirmed by Ponceau staining. Blocking was done with 5% nonfat milk in TBS containing 0.1% Tween 20 (TBST). Immunoblotting was done with phospho-specific antibodies to phospho-AKT-Ser[473], phospho-AKT-Thr[308], and phospho-IGF1R-1135 (all from Cell Signaling Technology), followed by incubation in the appropriate horseradish peroxidase–conjugated secondary antibody (Pierce Biotechnology) and enhanced chemiluminescence detection (GE Healthcare). Membranes were placed in stripping buffer [62.5 mmol/L Tris-HCl (pH 6.8), 2% SDS, 0.1 mol/L β-mercaptoethanol] at 50°C for 15 minutes, followed by washing of the membrane with TBST. The absence of residual chemiluminescence on the membrane was confirmed by exposure of autoradiograph film. The stripped membranes were probed with antibodies to

AKT and IGF1R (both from Santa Cruz Biotechnology). For some experiments, both stripped and new membranes of the same lysates were used to confirm that immunoreactivity was similar when using stripped versus new membranes. All films were scanned and saved in unmodified TIFF format. Densitometry was done using ImageJ software. Phospho-AKT expression was normalized to total AKT and shown as the fold change relative to untreated cells. Anti–glyceraldehyde-3-phosphate dehydrogenase antibody (Cell Signaling Technology) was used to show equal protein loading.

RNA isolation, reverse transcription, and quantitative real-time PCR

Cell lysates were homogenized using QIAshredder columns (Qiagen, Inc.), and total RNA was isolated by RNeasy Mini kit (Qiagen) with on-column DNase I (Qiagen) treatment. RNA quantity, purity, and integrity were evaluated using the NanoDrop spectrophotometer (Fisher Thermo Scientific) and Agilent Bioanalyzer (Agilent Technologies). Complementary DNA was synthesized from 1 μg of total RNA using SuperScript III reverse transcriptase (Invitrogen).

To determine the expression level of IGF2, quantitative real-time PCR was done using an Applied Biosystems 7900HT Fast Real-Time PCR System. Each reaction used 1/20th of the cDNA reaction, forward and reverse primers at a final concentration of 200 nmol/L, and Power SYBR (Applied Biosystems) diluted in Ultrapure water (Invitrogen) to 1× final concentration. Forward and reverse primer sequences used for IGF1, IGF2, and cyclophilin B were previously validated (16–19). Melting curve analysis was done to confirm a single amplicon corresponding to the PCR product size for each reaction. Real-time PCR results were analyzed by the $2^{-\Delta\Delta Ct}$ method to quantify the relative mRNA expression level, as previously described (20).

Cytotoxicity assay

Cells were seeded in 96-well plates at 2,000 per well and, after 24 hours, treated with serial dilutions of Taxol for an additional 72 hours. For drug combination experiments, cells were treated with serial dilutions of Taxol, with or without the addition NVP-AEW541 at 1 μmol/L. After 72 hours of treatment, the relative cell number in each well was determined using the sulforhodamine B (SRB) assay. Cell growth was expressed as %, defined as the ratio of the absorbance in the treated well compared with the control well × 100, as previously described (21). Using CalcuSyn software, dose-effect curves were generated, and the drug concentrations corresponding to a 50% decrease in cell number (IC_{50}) were determined.

IGF2 depletion by small interfering RNA

Stealth IGF2 small interfering RNA (siRNA) oligonucleotides and nontargeting Negative Control High-GC Stealth siRNA were obtained from Invitrogen. The RNAiMax Lipofectamine (Invitrogen) reverse transfection was done according to the manufacturer's recommended protocol

in 60-mm^2 dishes using the experimentally determined optimal siRNA oligonucleotide concentration of 20 nmol/L. After 24 hours of incubation in antibiotic-free Opti-MEM (Invitrogen) with 10% fetal bovine serum, cells were trypsinized and used for the experiments described below. For each experiment, IGF2 siRNA and negative control siRNA transfections were done in parallel.

To determine the effect of IGF2 knockdown on cell proliferation and Taxol sensitivity, IGF2 siRNA– or control siRNA–transfected cells were seeded 24 hours after transfection into six-well plates at a density of 1.5×10^4/mL and then treated with Taxol, or DMSO, for 72 hours. Adherent cells from each of three replicate wells per treatment were trypsinized and counted on a Coulter counter. The cell proliferation was determined and expressed relative to control siRNA–transfected cells.

To confirm the efficiency of RNA knockdown, three replicate wells of transfected cells from each six-well plate were harvested at the termination of the experiment (96 h after transfection) for RNA isolation and quantitative real-time PCR analysis of IGF2 expression.

Clinical specimens

This study was reviewed and approved by the Institutional Review Boards of the Albert Einstein College of Medicine and the University of New Mexico Health Sciences Center. Formalin-fixed, paraffin-embedded tumor specimens from 134 patients diagnosed with epithelial ovarian carcinoma (EOC) or low malignant potential (LMP) epithelial tumors, treated at the University of New Mexico Cancer Center between March 1996 and June 2006, were retrieved from the Human Tissue Repository. Specimens were obtained at the time of primary surgery. After secondary pathology review, a tissue microarray was constructed, containing two cores from each specimen obtained at the time of primary surgery. Tissue cores were absent in 19 cases, leaving 115 cases available for evaluation. Pertinent clinical data were abstracted, and a deidentified database was created. Investigators were blinded to clinical data until completion of staining and scoring.

Immunohistochemistry

Immunohistochemistry was done using a rabbit polyclonal antibody directed at the IGF2 ligand (Abcam, Inc.). The optimal blocking and primary antibody conditions were determined using placental tissue. In brief, Target Retrieval Solution, Citrate pH 6 (Dako North America, Inc.) was used for antigen retrieval, TBS containing 5% goat serum and 2% bovine serum albumin was used for blocking, and the primary antibody was used at a 1:100 dilution with an incubation of 1 hour at room temperature. Secondary antibody and detection were done using the Dako Envision+ Polymer System (Dako North America), followed by counterstaining with hematoxylin. Staining of all tissue microarray slides was done concurrently with staining of positive and negative control sections. Representative placenta sections are shown following staining with the IGF2 antibody or with IGF2 antibody that
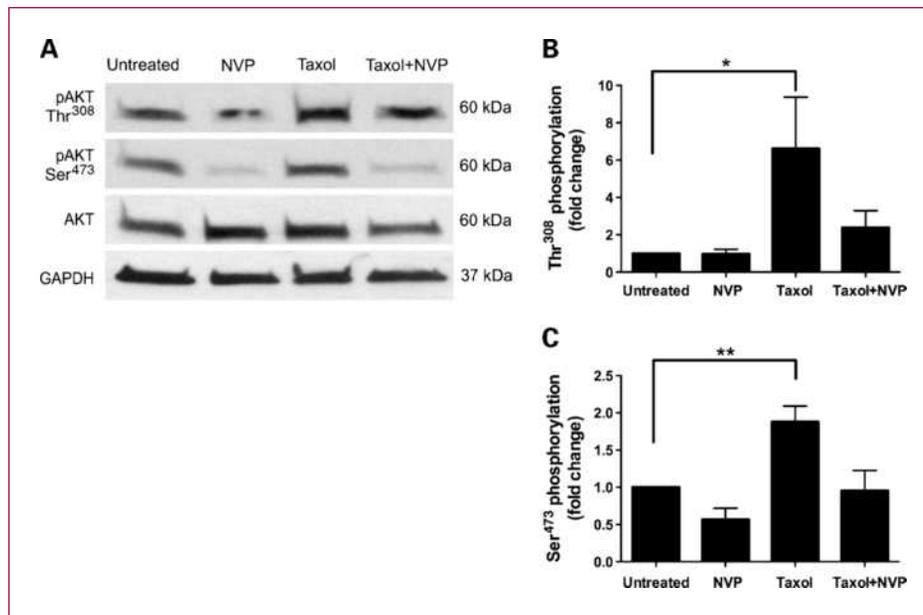
Fig. 1. Effect of Taxol treatment on AKT phosphorylation. A2780 cells were maintained in complete media containing 10% fetal bovine serum and treated for 24 h with Taxol (5 nmol/L), NVP-AEW541 (1 μmol/L), or both drugs concurrently. Immunoblotting was done to determine the effect of Taxol treatment on AKT phosphorylation. A, representative immunoblots are shown for phospho-AKT (pAKT; Thr[308]) and phospho-AKT (Ser[473]), along with the corresponding total AKT and glyceraldehyde-3-phosphate dehydrogenase (GAPDH) immunoblots. B, the relative level of AKT phosphorylation at Thr[308], as determined by densitometry, is shown in the graph. Columns, mean of four independent experiments; bars, SE. *, $P < 0.05$, one-way ANOVA, Dunnett post test. C, the relative level of AKT phosphorylation at Ser[473], as determined by densitometry, is shown in the graph. Columns, mean of seven independent experiments; bars, SE. **, $P < 0.01$, one-way ANOVA, Dunnett post test.1

was preabsorbed with recombinant IGF2 (Supplementary Fig. S5). Representative stained ovarian tissue sections were photographed on a Zeiss Axioskop II, and images shown in Fig. 5 depict the TIFF image files without modifications, other than cropping of the size. To evaluate assay reproducibility, IGF2 immunohistochemistry was repeated on an independently constructed tissue microarray that contained distinct tissue cores from 53 of the tumor specimens comprising the study population.

A gynecologic pathologist (T.M.H.), who was blinded to all clinical data, graded the cytoplasmic staining intensity (0, negative; 1+, weak; 2+, moderate; 3+, strong) and the percentage of tumor cells with positive staining (1-100%). The H-score is defined as the product of the staining intensity and the percentage of positive staining; the mean H-score for each tumor was determined from the corresponding tissue cores.

Statistical analysis

For cell line experiments, numerical values (drug concentrations, combination index, and mRNA levels) are expressed as the mean ± SD, or mean ± SE, as indicated. The differences in mean values between two groups were statistically analyzed using the two-tailed t test, whereas the differences in mean values between multiple groups were analyzed using one-way or two-way ANOVA with the appropriate post test, as indicated.

For analysis of IGF2 expression in the ovarian tumor tissues, IGF2 expression was categorized as high or low

using the median IGF2 H-score, and the χ^2 or Fisher's exact tests were used to determine the association of IGF2 expression with clinical and pathologic variables. Correlation of IGF2 H-scores obtained using two independently constructed and stained tissue microarrays was assessed by Spearman rank correlation. Survival analysis was done to study the effect of IGF2 expression on overall and disease-free death events using the Cox proportional hazards regression. Additional adjustment for age, grade, stage, extent of cytoreduction, performance status, and chemotherapy was achieved by including these variables in the Cox models. A predictor was considered as a potential candidate for the final model if the log-rank test of equality across strata had a P value of <0.25 in a univariate analysis. During final multivariate Cox model building, all the potential predictors were included in the model and the Wald test was used to measure the statistical significance of hazard ratios. All the possible interactions were tested and proportional hazards assumptions were checked. No significant interactions were found, and the final model was stratified on the nonproportional predictors.

All P values are two-tailed, and P values <0.05 were considered statistically significant.

Results

Activation of AKT by Taxol

The effect of Taxol treatment on AKT activation in A2780 cells was evaluated by immunoblot analysis. Initially,

a dose-response experiment was done to evaluate a range of Taxol concentrations (1, 5, and 50 nmol/L). The 5 nmol/L concentration produced the largest effect on AKT phosphorylation at 24 hours (data not shown); therefore, subsequent experiments used this drug concentration. As shown in Fig. 1, Taxol (5 nmol/L) treatment for 24 hours resulted in increased AKT phosphorylation at the critical residues for activation, Thr[308] and Ser[473]. The mean fold change in phosphorylation level after Taxol treatment, compared with basal phosphorylation level, was 8.5- and 2-fold for Thr[308] and Ser[473], respectively. ERK phosphorylation was not appreciably altered by Taxol treatment in these cells (data not shown).

To determine whether Taxol-induced AKT phosphorylation is dependent on IGF1R activation, the small-molecule IGF1R tyrosine kinase inhibitor NVP-AEW541 was used. With regard to selectivity, NVP-AEW541 is a 27-fold more potent inhibitor of the IGF1R kinase compared with inhibition of the insulin receptor kinase, >50-fold more potent compared with inhibition of c-Kit, and >100-fold more potent compared with inhibition of HER1, platelet-derived growth factor receptor, and Bcr-Abl (14). We evaluated a range of concentrations of NVP-AEW541 (0.1-10 μmol/L) for the ability to disrupt IGF1R signaling in ovarian carcinoma cells. NVP-AEW541 at 1 μmol/L effectively abrogates IGF2-induced IGF1R autophosphorylation and downstream AKT phosphorylation, and this concentration was used for subsequent experiments (Supplementary Fig. S1).

As shown in Fig. 1, Taxol-induced AKT phosphorylation was inhibited by concurrent treatment with the IGF1R inhibitor NVP-AEW541. Our results indicate that Taxol treatment results in increased AKT phosphorylation and that phosphorylation of AKT due to Taxol treatment requires IGF1R tyrosine kinase activity.
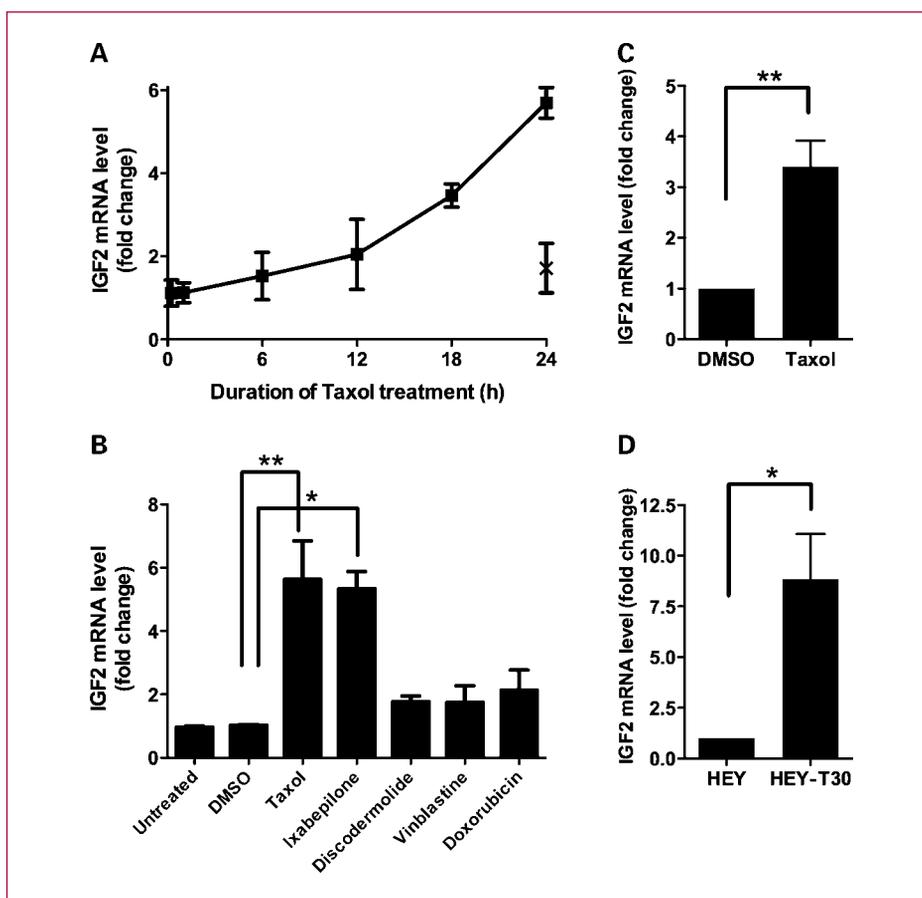

Fig. 2. Taxol-induced IGF2 mRNA expression. A, the time course of IGF2 expression following Taxol treatment (5 nmol/L) in A2780 cells is depicted with squares and a solid connecting line. The IGF2 mRNA level after baccatin treatment (5 nmol/L) for 24 h is also shown on the graph, marked by an X. Points, mean of two independent experiments, each done in triplicate; bars, SE. B, A2780 cells were treated for 24 h with vehicle alone (DMSO) or with cytotoxic drugs at their equipotent molar concentrations. The IGF2 mRNA level is expressed as fold change relative to untreated cells. Columns, mean of two independent experiments, each done in triplicate; bars, SE. *, $P < 0.05$; **, $P < 0.01$, one-way ANOVA, Dunnett post test. C, HEY cells were treated with vehicle alone (DMSO) or Taxol (5 nmol/L) for 24 h. The IGF2 mRNA level, determined by reverse transcription quantitative real-time PCR, is expressed as fold change relative to untreated cells in complete growth medium. Columns, mean of three independent experiments, each done in triplicate; bars, SE. **, $P < 0.01$, t test. D, IGF2 mRNA expression in Taxol-resistant HEY-T30 cells, determined by reverse transcription quantitative real-time PCR, is expressed as fold change relative to HEY parental cells. Columns, mean of three independent experiments, each done in triplicate; bars, SE. *, $P < 0.05$, t test.

IGF2 regulation by Taxol

To investigate whether the observed IGF1R activation is mediated by autocrine signaling, the effect of Taxol treatment on the expression of IGF1 and IGF2 mRNAs was quantified in A2780 cells. A dose-response experiment was done to evaluate the effect of different Taxol concentrations (1, 5, 20, and 50 nmol/L) on IGF2 mRNA levels. Concordant with the immunoblot results, 5 nmol/L Taxol produced the greatest increase in IGF2 mRNA expression (data not shown). Following Taxol treatment (5 nmol/L), IGF2 mRNA levels progressively increased over 24 hours (Fig. 2A). In contrast, cells treated with baccatin III, an inactive Taxol analogue that does not bind to or stabilize microtubules (22), did not alter IGF2 mRNA levels compared with untreated cells. IGF1 mRNA expression was unchanged after Taxol treatment (data not shown).

To evaluate whether treatment with other cytotoxic compounds induces IGF2 mRNA expression, A2780 cells were treated for 24 hours with each of several microtubule-interacting drugs and other compounds at their approximately equipotent drug concentrations (as determined by SRB proliferation assays), and IGF2 mRNA levels were measured (Fig. 2B). Treatment with the microtubule-stabilizing agent (MSA) ixabepilone (10 nmol/L), an epothilone compound with a chemical structure distinct from Taxol, resulted in an increase in IGF2 mRNA expression to a similar degree as Taxol. However, treatment with discodermolide (20 nmol/L), also a MSA but with a more complex mechanism of action (23, 24), did not significantly induce IGF2 mRNA at this time point. Treatment with the microtubule-destabilizing agent vinblastine (5 nmol/L) or the DNA-intercalating agent doxorubicin (50 nmol/L) did not result in significant IGF2 upregulation. These findings suggest that IGF2 upregulation by Taxol does not occur as a generalized response to cytotoxic drugs but may require a specific interaction with microtubules that is shared between Taxol and ixabepilone.

Evaluation of paired sensitive and resistant HEY ovarian cancer cells

The Taxol-resistant cell line HEY-T30 was developed in our laboratory by repeated exposure of HEY ovarian carcinoma cells to Taxol. Like A2780 cells, HEY ovarian carcinoma cells exhibit upregulation of IGF2 mRNA levels following Taxol treatment for 24 hours (Fig. 2C). The Taxol-resistant HEY-T30 cells exhibit significantly elevated IGF2 mRNA levels compared with the parental HEY cells (Fig. 2D). Under either normal growth or serum starvation
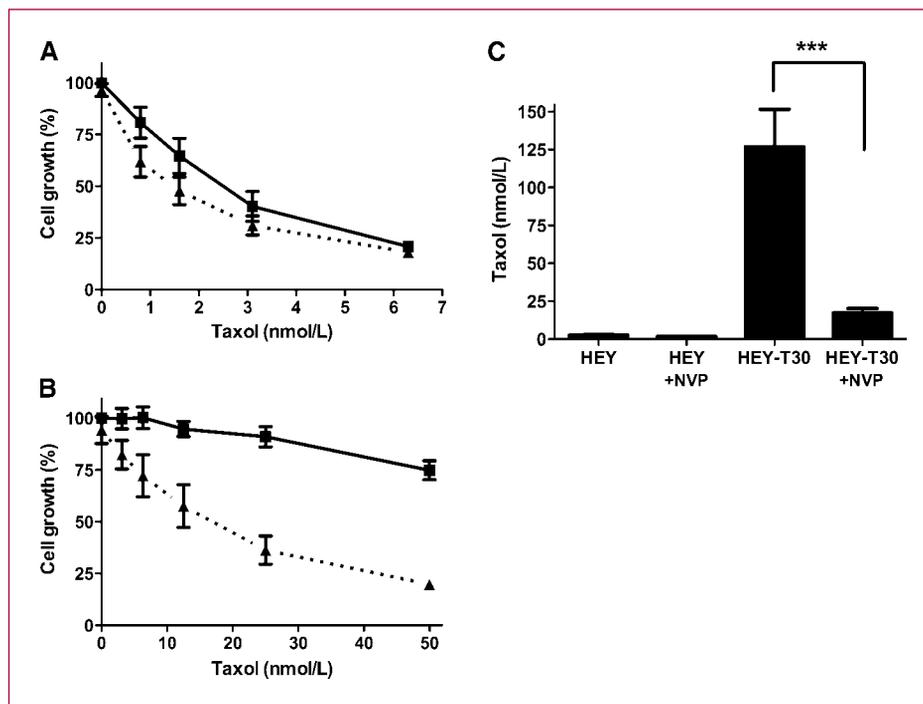

Fig. 3. Potentiation of Taxol treatment by the IGF1R inhibitor NVP-AEW541. Cytotoxicity assays for HEY and HEY-T30 ovarian carcinoma cells were done using the SRB method to determine the effect of Taxol treatment alone or with concurrent NVP-AEW541. A, HEY parental cells: the cell number relative to untreated cells, expressed as cell growth (%), is plotted over a range of Taxol concentrations. Treatment with Taxol alone is depicted with squares and solid lines, compared with combination treatment with Taxol plus NVP-AEW541 1 μmol/L, depicted with triangles and dotted lines. The cell growth (%) resulting from NVP-AEW541 (1 μmol/L) alone is plotted on the Y axis (triangle). $P < 0.05$, two-way ANOVA. B, HEY-T30 resistant cells: the cell number relative to untreated cells, expressed as cell growth (%), is plotted over a range of Taxol concentrations, as in A. The cell growth (%) resulting from NVP-AEW541 (1 μmol/L) alone is plotted on the Y axis (triangle). $P < 0.001$, two-way ANOVA. C, for each cell line, the IC_{50} concentration of Taxol alone or with concurrent NVP-AEW541 (1 μmol/L) is plotted in the bar graph. Columns, mean of at least three independent experiments with six replicates each; bars, SE. $P < 0.0001$, one-way ANOVA, Bonferroni post test.

conditions, constitutive IGF1R phosphorylation is observed in HEY-T30 cells, whereas parental HEY cells do not exhibit constitutive IGF1R phosphorylation (Supplementary Fig. S2). Cross-resistance to cisplatin, a platinum DNA-damaging chemotherapy drug, is not observed in HEY-T30 cells (Supplementary Fig. S3).

The Taxol concentration that results in 50% growth inhibition (IC_{50}) for parental and resistant cells is shown in Fig. 3. We next assessed whether inhibition of IGF1R alters Taxol sensitivity in HEY and HEY-T30 cells. The growth inhibition resulting from combination drug treatment with Taxol and concurrent NVP-AEW541 was evaluated and compared with the effect of either drug alone (Fig. 3). As in the previous experiment, NVP-AEW541 was used at a concentration of 1 μmol/L, a concentration that effectively blocks IGF1R phosphorylation. As a single agent, NVP-AEW541 (1 μmol/L) alone had a minimal effect on cell growth in either cell line. In the parental HEY cells, treatment with NVP-AEW541 (1 μmol/L) modestly potentiated the effect of Taxol. In these cells, the IC_{50} for Taxol is 2.6 nmol/L; however, in the presence of NVP-AEW541, it is 1.7 nmol/L. The potentiation of Taxol efficacy by NVP-AEW541 in the resistant HEY-T30 cells was more dramatic. In the resistant cells, the IC_{50} for Taxol is 106 nmol/L, whereas in the presence of NVP-AEW541 it decreases to 17 nmol/L, representing a >6-fold sensitization to Taxol. Thus, IGF1R inhibition was efficacious in sensitizing ovarian cancer cells to Taxol in this model of acquired drug resistance.

We have evaluated three additional ovarian carcinoma cell lines made resistant to Taxol and other MSAs in our laboratory. As determined by SRB assay, the A2780-Tx15 cell line is 20-fold resistant to Taxol, the HEY-BMS20 cell line is 3-fold resistant to ixabepilone, and the OVCAR8-D30 cell line is 2-fold resistant to discodermolide. Each of these resistant cell lines is significantly sensitized to MSA treatment by concurrent IGF1R inhibition using 1 μmol/L NVP-AEW541.

IGF2 knockdown in Taxol-resistant cells

IGF1R inhibition would be expected to block signaling transduced not only by IGF2 but also by IGF1 ligand binding. Therefore, to determine whether inhibition of IGF2-transduced signaling alone is sufficient to sensitize ovarian cancer cells to Taxol, IGF2 depletion by siRNA was examined. The parental HEY cells and the Taxol-resistant HEY-T30 cells were transfected with IGF2 siRNA or control siRNA. As determined by real-time PCR, the efficacy of IGF2 mRNA knockdown by IGF2 siRNA was decreased by ~90% at 48 and 96 hours; immunoblotting confirmed that IGF2 protein expression was decreased by ~70% by IGF2 siRNA treatment (Supplementary Fig. S4).

For each cell line, the proliferation and the sensitivity of the IGF2-depleted cells to Taxol were compared with control siRNA–transfected cells. In parental HEY cells (Fig. 4A), IGF2 depletion does not significantly affect the cell growth, nor does it significantly potentiate the effect of Taxol in these cells, compared with control siRNA transfec-
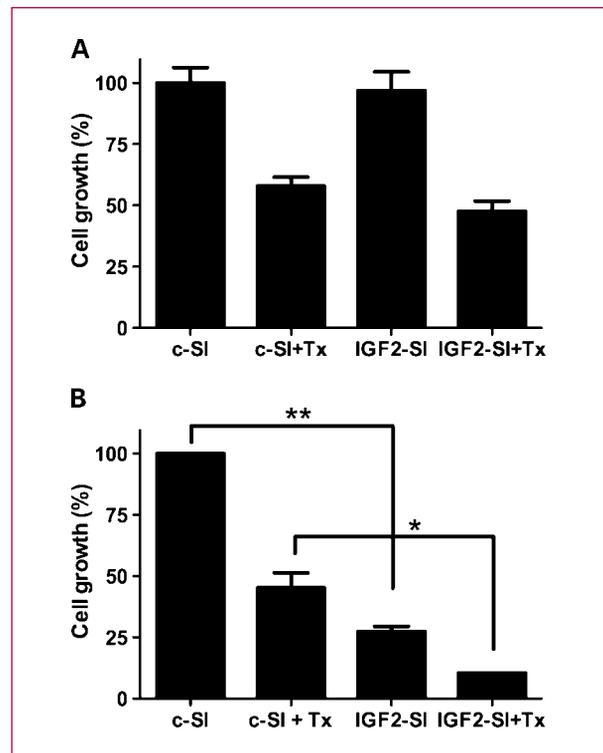

Fig. 4. Effect of IGF2 depletion by siRNA transfection in HEY (A) and HEY-T30 cells (B). IGF2 siRNA transfection was used to evaluate the effect of IGF2 depletion on cell proliferation and Taxol (Tx) sensitivity. Cells were transfected with IGF2 siRNA (IGF2-SI) or control siRNA (c-SI). Twenty-four hours after transfection, cells were counted, reseeded, and incubated for an additional 72 h, with or without the addition of Taxol at the IC_{50} concentration of Taxol for each cell line, followed by cell counting. Cell numbers are expressed as % cell growth relative to DMSO-treated, control siRNA–transfected cells. Columns, mean of two independent experiments, each done in triplicate for HEY parental cells (A) and HEY-T30 cells (B); bars, SE. *, $P < 0.05$; **, $P < 0.01$, one-way ANOVA, Bonferroni post test.

tion. In contrast, the effect of IGF2 depletion in the resistant HEY-T30 cells is substantial (Fig. 4B). Unlike IGF1R inhibition, which alone minimally affects cellular proliferation of HEY-T30 cells, IGF2 depletion by siRNA robustly suppressed cellular proliferation. The relative cell number following IGF2 siRNA transfection was 27% compared with control siRNA–transfected cells, corresponding to an ~4-fold reduction in cell number ($P < 0.01$). Treatment of IGF2-depleted HEY-T30 cells using approximately the IC_{50} concentration of Taxol (100 nmol/L) was highly efficacious. As shown in Fig. 4B, IGF2 siRNA plus Taxol treatment resulted in 10% cell growth after a 72-hour incubation compared with 45% cell growth following control siRNA plus Taxol treatment ($P < 0.05$).

IGF2 expression in epithelial ovarian tumors

To assess the potential clinical application of these findings, IGF2 protein expression was analyzed in primary ovarian tumors. The clinical and pathologic characteristics of the study population are shown in Table 1. Thirty-six

(31.3%) patients had epithelial ovarian tumors of LMP, whereas 79 (68.7%) had invasive EOC. Patients with EOC were older ($P = 0.001$) and were more likely to have advanced-stage disease ($P < 0.001$). The distribution of histologic types differed between the LMP and the EOC groups ($P < 0.001$). In the EOC group, serous histology (55.7%) was the most frequent histology. Mucinous histology was more frequent in the LMP group than in the EOC group (47.2% versus 13.9%).

Representative tissue sections of benign and malignant clinical specimens showing a range of IGF2 protein expression, with corresponding H-scores noted in the figure legends, are shown in Fig. 5. Positive and negative control sections used for quality assurance are shown in Supplementary Fig. S5. To assess potential batch effects and biological variation due to tissue sampling, a second tissue microarray was used that included distinct tissue cores from 53 tumors from the original study population. The correlation of IGF2 H-scores from the two independently constructed and stained tissue microarrays was high (Spearman rank correlation, $R = 0.664$).

Table 2 depicts the association of IGF2 expression with selected clinical and pathologic variables. IGF2 tumor expression was not correlated with age or ethnicity. As shown in Fig. 6A, IGF2 expression was significantly associated with International Federation of Gynecologists and Obstetricians (FIGO) stage, with higher expression in advanced-stage tumors compared with early-stage tumors ($P < 0.001$). The histologic subtypes showed distinct patterns of expression (Fig. 6B): mucinous tumors had lower IGF2 expression compared with serous or endometrioid tumors ($P = 0.011$). As shown in Fig. 6C, IGF2 expression varied significantly with tumor grade, with higher expression observed in invasive epithelial ovarian cancers compared with borderline ovarian tumors ($P = 0.003$).

On univariate survival analysis (Fig. 6D), high IGF2 expression was significantly associated with reduced disease-free survival ($P = 0.03$). Age ($P = 0.02$), grade ($P < 0.0001$), stage ($P < 0.0001$), extent of cytoreduction ($P < 0.0001$), performance status ($P = 0.0002$), and chemotherapy ($P = 0.0002$), but not race or histology, were risk factors associated with disease-free survival on univariate analysis. When LMP tumors were excluded from the analysis, the association of IGF2 expression and disease-free survival was no longer statistically significant (Fig. 6E).

Table 1. Characteristics of the study population

Variable	LMP, *n* (%)	EOC, *n* (%)	Total, *n* (%)	*P*
Age (y)				0.001
≤50	22 (61.1)	23 (29.1)	45 (39.1)	
>50	14 (38.9)	56 (70.9)	70 (60.9)	
Race/ethnicity				0.142
Non-Hispanic White	21 (58.3)	36 (45.6)	57 (49.6)	
Hispanic	11 (30.6)	28 (35.4)	39 (33.9)	
American Indian	2 (5.6)	14 (17.7)	16 (13.9)	
Black	1 (2.8)	1 (1.3)	2 (1.7)	
Asian	1 (2.8)	0	1 (0.9)	
FIGO stage				<0.001
I	32 (88.9)	24 (30.4)	56 (48.7)	
II	2 (5.6)	7 (8.9)	9 (7.8)	
III	2 (5.6)	38 (48.1)	40 (34.8)	
IV	0	10 (12.7)	10 (8.7)	
Histology				<0.001
Serous	17 (47.2)	44 (55.7)	61 (53.0)	
Mucinous	17 (47.2)	11 (13.9)	28 (24.3)	
Endometrioid	0	6 (7.6)	6 (5.2)	
Other	2 (5.6)	18 (22.8)	20 (17.4)	
Grade				N/A
0	36 (100.0)	0	36 (31.3)	
1	0	12 (15.2)	12 (10.4)	
2	0	19 (24.1)	19 (16.5)	
3	0	48 (60.8)	48 (41.7)	
Total	36	79	115	

NOTE: Race/ethnicity as defined by Surveillance Epidemiology and End Results coding.
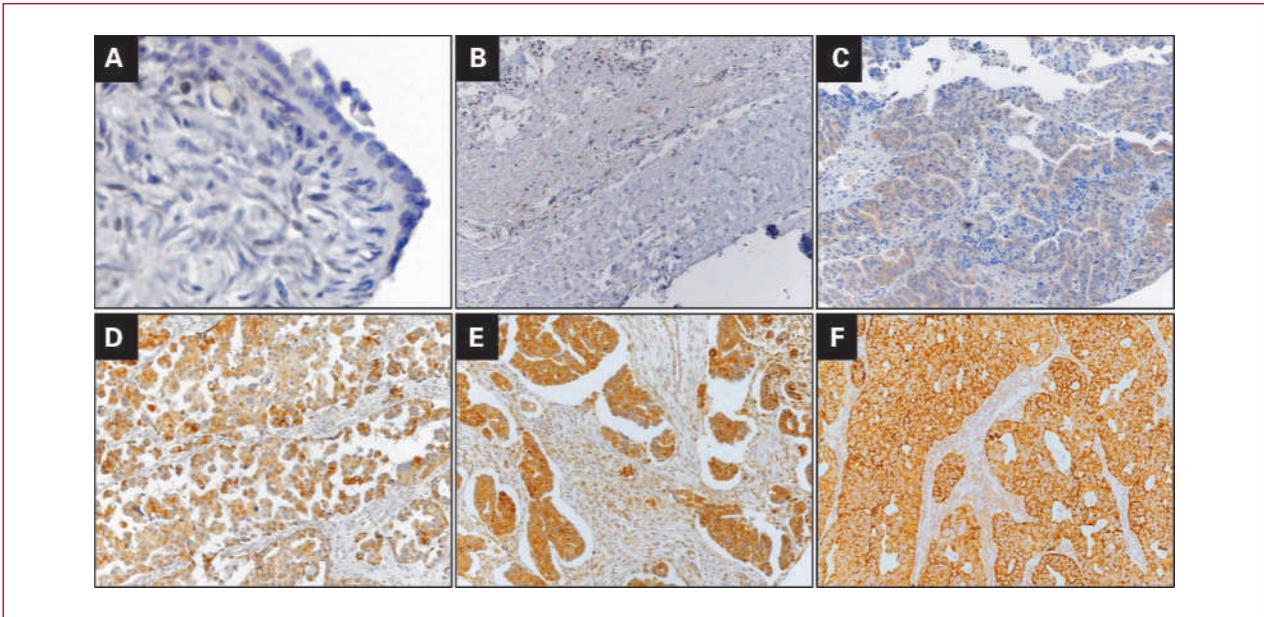Abbreviation: N/A, not applicable.

Fig. 5. Representative images of IGF2 immunohistochemical staining. A, absence of staining in the surface epithelium of a normal ovary. Magnification, ×40. B, extremely low staining in a stage I mucinous borderline tumor (H-score = 0.5). C, low staining in a stage III, grade 1 serous carcinoma (H-score = 75). D, medium staining in a stage III, grade 3 serous carcinoma (H-score = 100). E, high staining in a stage III, grade 3 adenocarcinoma, not otherwise specified (H-score = 250). F, high staining in a stage III, grade 3 serous carcinoma (H-score 300).

On multivariate analysis, stage ($P = 0.001$), extent of cytoreduction ($P = 0.002$), and grade ($P = 0.04$) were independently associated with disease-free survival.

With regard to overall survival, there have been 29 deaths. There have been 12 deaths (among 60 patients; 20%) in the low IGF2 group compared with 17 deaths (among 55 patients; 31%) in the high IGF2 group; the effect of IGF2 expression on overall survival was not significant on univariate analysis ($P = 0.19$). Age ($P = 0.005$), grade ($P < 0.0001$), stage ($P < 0.0001$), extent of cytoreduction ($P < 0.0001$), performance status ($P < 0.0001$), and chemotherapy ($P = 0.009$) were risk factors associated with overall survival on univariate analysis. For multivariate analysis, stratification by grade (LMP versus EOC) was done, as no deaths occurred in the LMP group. On multivariate survival analysis, stage ($P = 0.007$), extent of cytoreduction ($P = 0.001$), and chemotherapy ($P = 0.0003$) were independently associated with overall survival.

Discussion

This study is the first, to our knowledge, to evaluate the role of the IGF signaling pathway in the response of ovarian carcinoma cells to Taxol. Our findings show that Taxol treatment results in upregulation of IGF2 expression associated with activation of AKT. As shown in a cell line model of acquired drug resistance in ovarian carcinoma, Taxol resistance is associated with elevated IGF2 expression, whereas IGF1R inhibition or IGF2 depletion restores drug sensitivity. In clinical tumor specimens, high IGF2 protein expression is significantly associated with poor prognostic factors for recurrence and death.

The pyrrolo[2,3-d]pyrimidine compound NVP-AEW541 used in this study and the closely related compound NVP-ADW742 were the first IGF1R-specific small-molecule tyrosine kinase inhibitors reported in the literature (14, 25). Using doses corresponding to specific inhibition of the IGF1R tyrosine kinase, we showed that NVP-AEW541 effectively blocks Taxol-induced AKT phosphorylation. Although NVP-AEW541 alone did not suppress proliferation in ovarian carcinoma cells, treatment with NVP-AEW541 significantly potentiated the effect of Taxol in both sensitive and resistant cells. Whereas the compound NVP-AEW541 is not undergoing clinical development at this time, a variety of small-molecule inhibitors and monoclonal antibodies that target the IGF1R are presently undergoing evaluation in clinical trials, and it is anticipated that one or more of these compounds may be approved for use in the clinic (13).

An alternate therapeutic strategy is to target the aberrantly expressed ligand, rather than its receptor. As IGF2 has been shown to bind not only the IGF1R but also the insulin receptor isoform A and hybrid IGF1R-insulin receptors, signaling by IGF2 could potentially circumvent the IGF1R in the presence of IGF1R-specific inhibitors (26, 27). In the present study, the combination of IGF2 depletion and Taxol was found to be highly effective at inhibiting cell growth in the setting of acquired drug resistance. Interestingly, IGF2 depletion alone resulted in potent suppression of proliferation distinct from the

minimal antiproliferative effect of IGF1R inhibition. The potent effect of IGF2 depletion suggests possible dependency on IGF2 for proliferation in these Taxol-resistant cells.

Previously, it was reported that PI3K and AKT inhibition could enhance sensitivity to Taxol (9, 28, 29). As PI3K and AKT are major downstream effectors of IGF1R activity, the concordant effects resulting from blockade at downstream targets in the IGF signaling cascade validate the findings of the present study. From a clinical perspective, significant metabolic toxicity has been encountered with direct AKT inhibition (29), highlighting a potential disadvantage to blockade at the downstream intracellular targets where multiple signaling pathways converge. Targeting a specific ligand-cell surface receptor may reduce these undesired effects on the physiology of normal cells. However, targeting at the receptor level, such as IGF1R or epidermal growth factor receptor inhibition, has been shown to promote activation of the reciprocal receptor in cancer cell lines via cross-talk mechanisms (30). Thus, it is likely that optimal combination treatment strategies will require consideration of compensatory feedback signals that occur in a cell-specific manner.

In the clinic, multidrug resistance is a hallmark of progressive ovarian cancer. In addition to Taxol, platinum compounds are widely used in the treatment of primary and recurrent ovarian cancer. Interestingly, it was recently reported that IGF1R inhibition may restore drug sensitivity in platinum-resistant ovarian cancer cells (31). Another study showed activity of an IGF1R-targeting antibody in a fluorouracil-resistant colorectal carcinoma cell line (32). With regard to tubulin-targeting agents, resistance to the MSA docetaxel was associated with predicted PI3K pathway activation, by gene expression profiling, in a variety of carcinoma cell lines (33). These studies, in conjunction with the present study, strongly support the relevance of the IGF pathway to chemotherapy resistance.

IGF2 upregulation has been implicated in carcinogenesis and disease progression in ovarian cancer. Previous studies used a gene expression microarray approach to identify IGF2 mRNA to be significantly overexpressed in ovarian cancer compared with benign ovary (34, 35). In addition, high IGF2 mRNA expression was associated with advanced stage, high grade, and poor survival in a cohort of patients

Table 2. IGF2 expression in LMP tumors and EOC

Variable	LMP tumors (n = 36)			EOC (n = 79)			Total (n = 115)		
	IGF2 low, n (%)	IGF2 high, n (%)	P	IGF2 low, n (%)	IGF2 high, n (%)	P	IGF2 low, n (%)	IGF2 high, n (%)	P
Age (y)			1.000			0.873			0.335
≤50	17 (60.7)	5 (62.5)		9 (28.1)	14 (29.8)		26 (43.3)	19 (34.5)	
>50	11 (39.3)	3 (37.5)		23 (71.9)	33 (70.2)		34 (56.7)	36 (65.5)	
Race/ethnicity			0.544			0.339			0.166
Non-Hispanic White	15 (53.6)	6 (75.0)		12 (37.5)	24 (51.1)		27 (45.0)	30 (54.6)	
Hispanic	10 (35.7)	1 (12.5)		14 (43.8)	14 (29.8)		24 (40.0)	15 (27.3)	
American Indian	1 (3.6)	1 (12.5)		5 (15.6)	9 (19.1)		6 (10.0)	10 (18.2)	
Black	1 (3.6)	0		1 (3.1)	0		2 (3.3)	0	
Asian	1 (3.6)	0		0	0		1 (1.7)	0	
FIGO stage			0.028			0.124			<0.001
I	27 (96.4)	5 (62.5)		12 (37.5)	12 (25.5)		39 (65.0)	17 (30.9)	
II	0	2 (25.0)		4 (12.5)	3 (6.4)		4 (6.7)	5 (9.1)	
III	1 (3.6)	1 (12.5)		15 (46.9)	23 (48.9)		16 (26.7)	24 (43.6)	
IV	0	0		1 (3.1)	9 (19.1)		1 (1.7)	9 (16.4)	
Histology			0.055			0.664			0.011
Serous	10 (35.7)	7 (87.5)		17 (53.1)	27 (57.4)		27 (45.0)	34 (61.8)	
Mucinous	16 (57.1)	1 (12.5)		6 (18.8)	5 (10.6)		22 (36.7)	6 (10.9)	
Endometrioid	0	0		3 (9.4)	3 (6.4)		3 (5.0)	3 (5.5)	
Other	2 (7.1)	0		6 (18.8)	12 (25.5)		8 (13.3)	12 (21.8)	
Tumor grade			N/A			0.933			0.003
0	28 (100.0)	8 (100.0)		0	0		28 (46.7)	8 (14.6)	
1	0	0		5 (15.6)	7 (14.9)		5 (8.3)	7 (12.7)	
2	0	0		7 (21.9)	12 (25.5)		7 (11.7)	12 (21.8)	
3	0	0		20 (62.5)	28 (59.6)		20 (33.3)	28 (50.9)	
Total	28	8		32	47		60	55	

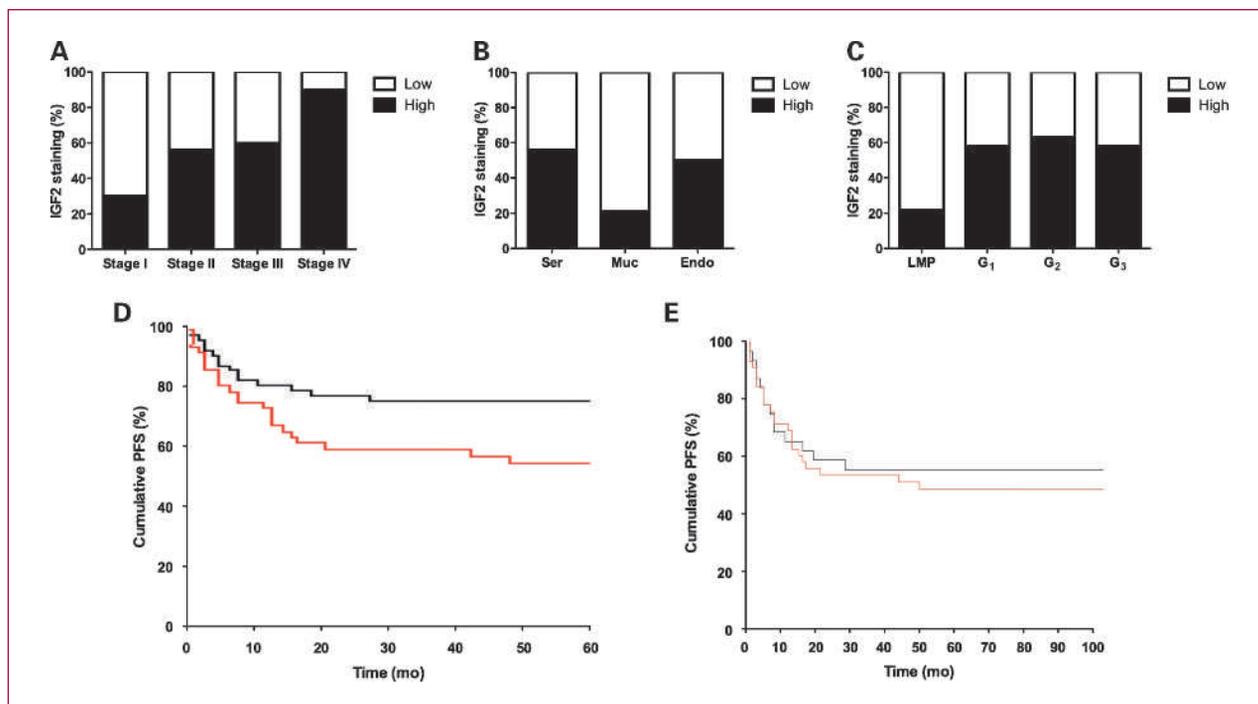NOTE: IGF2 low, H-score ≤ 105; IGF2 high, H-score > 105.

Fig. 6. Correlation between IGF2 expression and clinicopathologic factors in ovarian tumors. A, IGF2 staining is correlated with FIGO stage, with higher frequency of IGF2 overexpression in advanced-stage tumors. $P < 0.001$, Fisher's exact test. B, serous (Ser) and endometrioid (Endo) histologic types are correlated with high IGF2 staining compared with mucinous (Muc) tumors. $P = 0.011$, χ^2 test. C, IGF2 staining is correlated with tumor grade, with LMP (borderline) tumors showing the lowest frequency of IGF2 overexpression. $P = 0.003$, Fisher's exact test. D, patients with high IGF2 expression (red line) had a significant reduction in progression-free survival (PFS) compared with patients with low IGF2 expression (black line). $P = 0.03$, log-rank test. E, when LMP tumors are excluded from the analysis, the association of IGF2 expression and progression-free survival is not statistically significant.

with serous epithelial ovarian cancer (36). Interestingly, IGF2 protein levels in the serum of patients with ovarian cancer were decreased compared with unaffected women (37, 38). The present study is, to our knowledge, the first to evaluate the significance of IGF2 expression at the protein level in ovarian tumors from patients. Consistent with the prior mRNA expression studies, high IGF2 protein expression was observed more frequently in patients with advanced-stage and high-grade tumors and was associated with clinical/pathologic predictors of worse prognosis. In the study sample, approximately half of the tumors were serous histology, which is the most common type of epithelial ovarian cancer; however, early-stage cancer, less common histologic types, and LMP tumors were also present at relatively high proportions in this cohort. Based on our findings, subsequent studies should prospectively evaluate IGF2 protein expression in primary and recurrent epithelial ovarian tumors for evaluation of its utility as a potential biomarker and to confirm its frequent overexpression in ovarian cancer. If IGF2 is found to be a useful biomarker, the standard methods used for IGF2 immunohistochemistry in this study are within the capability of many surgical pathology laboratories and therefore readily translatable to clinical application.

In summary, activation of autocrine IGF signaling occurs following Taxol treatment of ovarian carcinoma cells and is observed in association with the acquisition of Taxol resistance. Inhibition of the IGF signaling pathway significantly potentiates Taxol efficacy and sensitizes drug-resistant cells. In primary ovarian tumors, high IGF2 expression is strongly associated with known clinicopathologic risk factors, including stage and grade, and its overexpression is associated with reduced disease-free survival. These findings strongly support the clinical relevance of the IGF pathway in ovarian cancer and suggest a potential therapeutic role for inhibitors of this pathway in the management of this disease.

Disclosure of Potential Conflicts of Interest

No potential conflicts of interest were disclosed.

Acknowledgments

Grant Support

References

1. Giannakakou P, Nakano M, Nicolaou KC, et al. Enhanced microtubule-dependent trafficking and p53 nuclear accumulation by suppression of microtubule dynamics. Proc Natl Acad Sci U S A 2002; 99:10855–60.
2. Horwitz SB. Taxol (paclitaxel): mechanisms of action. Ann Oncol 1994;5 Suppl 6:S3–6.
3. Rao S, Orr GA, Chaudhary AG, Kingston DG, Horwitz SB. Characterization of the taxol binding site on the microtubule. 2-(*m*-Azidobenzoyl)taxol photolabels a peptide (amino acids 217-231) of β-tubulin. J Biol Chem 1995;270:20235–8.
4. Schiff PB, Fant J, Horwitz SB. Promotion of microtubule assembly *in vitro* by taxol. Nature 1979;277:665–7.
5. Jordan MA, Wilson L. Microtubules as a target for anticancer drugs. Nat Rev Cancer 2004;4:253–65.
6. Orr GA, Verdier-Pinard P, McDaid H, Horwitz SB. Mechanisms of Taxol resistance related to microtubules. Oncogene 2003;22: 7280–95.
7. McDaid HM, Horwitz SB. Selective potentiation of paclitaxel (taxol)-induced cell death by mitogen-activated protein kinase kinase inhibition in human cancer cell lines. Mol Pharmacol 2001;60:290–301.
8. McDaid HM, Lopez-Barcons L, Grossman A, et al. Enhancement of the therapeutic efficacy of taxol by the mitogen-activated protein kinase kinase inhibitor CI-1040 in nude mice bearing human heterotransplants. Cancer Res 2005;65:2854–60.
9. Mabuchi S, Ohmichi M, Kimura A, et al. Inhibition of phosphorylation of BAD and Raf-1 by Akt sensitizes human ovarian cancer cells to paclitaxel. J Biol Chem 2002;277:33490–500.
10. Gotlieb WH, Bruchim I, Gu J, et al. Insulin-like growth factor receptor I targeting in epithelial ovarian cancer. Gynecol Oncol 2006;100: 389–96.
11. Dudek H, Datta SR, Franke TF, et al. Regulation of neuronal survival by the serine-threonine protein kinase Akt. Science 1997;275:661–5.
12. Kulik G, Klippel A, Weber MJ. Antiapoptotic signalling by the insulin-like growth factor I receptor, phosphatidylinositol 3-kinase, and Akt. Mol Cell Biol 1997;17:1595–606.
13. Rodon J, DeSantos V, Ferry RJ, Jr., Kurzrock R. Early drug development of inhibitors of the insulin-like growth factor-I receptor pathway: lessons from the first clinical trials. Mol Cancer Ther 2008;7:2575–88.
14. Garcia-Echeverria C, Pearson MA, Marti A, et al. *In vivo* antitumor activity of NVP-AEW541—a novel, potent, and selective inhibitor of the IGF-IR kinase. Cancer Cell 2004;5:231–9.
15. Yang CP, Horwitz SB. Taxol mediates serine phosphorylation of the 66-kDa Shc isoform. Cancer Res 2000;60:5171–8.
16. Lu L, Katsaros D, Wiley A, et al. Promoter-specific transcription of insulin-like growth factor-II in epithelial ovarian cancer. Gynecol Oncol 2006;103:990–5.
17. Lu L, Katsaros D, Wiley A, et al. The relationship of insulin-like growth factor-II, insulin-like growth factor binding protein-3, and estrogen receptor-α expression to disease progression in epithelial ovarian cancer. Clin Cancer Res 2006;12:1208–14.
18. Matsuyama R, Togo S, Shimizu D, et al. Predicting 5-fluorouracil chemosensitivity of liver metastases from colorectal cancer using primary tumor specimens: three-gene expression model predicts clinical response. Int J Cancer 2006;119:406–13.
19. Alexiadis M, Mamers P, Chu S, Fuller PJ. Insulin-like growth factor, insulin-like growth factor-binding protein-4, and pregnancy-associated plasma protein-A gene expression in human granulosa cell tumors. Int J Gynecol Cancer 2006;16:1973–9.
20. Bookout AL, Cummins CL, Mangelsdorf DJ, Pesola JM, Kramer MF. High-throughput real-time quantitative reverse transcription PCR. Curr Protoc Mol Biol 2006;Chapter 15:Unit 15.8.
21. Skehan P, Storeng R, Scudiero D, et al. New colorimetric cytotoxicity assay for anticancer-drug screening. J Natl Cancer Inst 1990;82:1107–12.
22. He L, Jagtap PG, Kingston DG, Shen HJ, Orr GA, Horwitz SB. A common pharmacophore for Taxol and the epothilones based on the biological activity of a taxane molecule lacking a C-13 side chain. Biochemistry 2000;39:3972–8.
23. Klein LE, Freeze BS, Smith AB III, Horwitz SB. The microtubule stabilizing agent discodermolide is a potent inducer of accelerated cell senescence. Cell Cycle 2005;4:501–7.
24. Huang GS, Lopez-Barcons L, Freeze BS, et al. Potentiation of taxol efficacy by discodermolide in ovarian carcinoma xenograft-bearing mice. Clin Cancer Res 2006;12:298–304.
25. Mitsiades CS, Mitsiades NS, McMullan CJ, et al. Inhibition of the insulin-like growth factor receptor-1 tyrosine kinase activity as a therapeutic strategy for multiple myeloma, other hematologic malignancies, and solid tumors. Cancer Cell 2004;5:221–30.
26. Pandini G, Frasca F, Mineo R, Sciacca L, Vigneri R, Belfiore A. Insulin/insulin-like growth factor I hybrid receptors have different biological characteristics depending on the insulin receptor isoform involved. J Biol Chem 2002;277:39684–95.
27. Sciacca L, Mineo R, Pandini G, Murabito A, Vigneri R, Belfiore A. In IGF-I receptor-deficient leiomyosarcoma cells autocrine IGF-II induces cell invasion and protection from apoptosis via the insulin receptor isoform A. Oncogene 2002;21:8240–50.
28. Hu L, Hofmann J, Lu Y, Mills GB, Jaffe RB. Inhibition of phosphatidylinositol 3′-kinase increases efficacy of paclitaxel in *in vitro* and *in vivo* ovarian cancer models. Cancer Res 2002;62:1087–92.
29. Luo Y, Shoemaker AR, Liu X, et al. Potent and selective inhibitors of Akt kinases slow the progress of tumors *in vivo*. Mol Cancer Ther 2005;4:977–86.
30. Haluska P, Carboni JM, TenEyck C, et al. HER receptor signaling confers resistance to the insulin-like growth factor receptor-I inhibitor, BMS-536924. Mol Cancer Ther 2008;7:2589–98.
31. Eckstein N, Serva K, Hildebrandt B, Politz A, von Jonquieres G, Wolf-Kummeth S. Hyperactivation of the insulin-like growth factor receptor I signaling pathway is an essential event for cisplatin resistance of ovarian cancer cells. Cancer Res 2009;69:2996–3003.
32. Dallas NA, Xia L, Fan F, Gray MJ, Gaur P, van Buren G. Chemoresistant colorectal cancer cells, the cancer stem cell phenotype, and increased sensitivity to insulin-like growth factor-I receptor inhibition. Cancer Res 2009;69:1951–7.
33. Potti A, Dressman HK, Bild A, et al. Genomic signatures to guide the use of chemotherapeutics. Nat Med 2006;12:1294–300.
34. Sawiris GP, Sherman-Baust CA, Becker KG, Cheadle C, Teichberg D, Morin PJ. Development of a highly specialized cDNA array for the study and diagnosis of epithelial ovarian cancer. Cancer Res 2002;62:2923–8.
35. Lancaster JM, Dressman HK, Whitaker RS, et al. Gene expression patterns that characterize advanced stage serous ovarian cancers. J Soc Gynecol Investig 2004;11:51–9.
36. Sayer RA, Lancaster JM, Pittman J, et al. High insulin-like growth factor-2 (IGF-2) gene expression is an independent predictor of poor survival for patients with advanced stage serous epithelial ovarian cancer. Gynecol Oncol 2005;96:355–61.
37. Visintin I, Feng Z, Longton G, et al. Diagnostic markers for early detection of ovarian cancer. Clin Cancer Res 2008;14:1065–72.
38. Mor G, Visintin I, Lai Y, et al. Serum protein markers for early detection of ovarian cancer. Proc Natl Acad Sci U S A 2005;102:7677–82.

AACR American Association
for Cancer Research

Clinical Cancer Research

Insulin-like Growth Factor 2 Expression Modulates Taxol Resistance and Is a Candidate Biomarker for Reduced Disease-Free Survival in Ovarian Cancer

Gloria S. Huang, Jurriaan Brouwer-Visser, Marissa J. Ramirez, et al.

Updated version	Access the most recent version of this article at: doi:10.1158/1078-0432.CCR-09-3233
Supplementary Material	Access the most recent supplemental material at: http://clincancerres.aacrjournals.org/content/suppl/2010/04/19/1078-0432.CCR-09-3233.DC1

Cited articles	This article cites 38 articles, 20 of which you can access for free at: http://clincancerres.aacrjournals.org/content/16/11/2999.full#ref-list-1
Citing articles	This article has been cited by 14 HighWire-hosted articles. Access the articles at: http://clincancerres.aacrjournals.org/content/16/11/2999.full#related-urls

E-mail alerts	Sign up to receive free email-alerts related to this article or journal.
Reprints and Subscriptions	To order reprints of this article or to subscribe to the journal, contact the AACR Publications Department at pubs@aacr.org.
Permissions	To request permission to re-use all or part of this article, use this link http://clincancerres.aacrjournals.org/content/16/11/2999. Click on "Request Permissions" which will take you to the Copyright Clearance Center's (CCC) Rightslink site.